systems possessing delocalized π-bonding between Si and S.

Conclusions

A combination of four principle factors are responsible for the thermodynamic stability of the π-bonded cation **1**.

(1) The positive charge enhances π-overlap and renders alternative π-bonded frameworks unfavorable, due to localization of charge on adjacent atoms.[8]

(2) The 10-π-electron count provides an inherent aromatic stabilization in addition to an efficient delocalization of the positive charge.

(3) Low basicity of anions, such as $AlCl_4^-$, prevents donation to the cation and subsequent covalent bond formation.[7] Nevertheless, the long-range nucleophilic contacts observed in the solid state are indicative of a degree of donation.

(4) The crystal lattice energy of the salt is expected to be greater than that of an alternative covalent Lewis adduct structure (**2**·$AlCl_3$). Although the energy difference may be small, it plays a significant role in the solid-state stability of the system, as demonstrated by the labile solution behavior.

The energy of the CC π-bond is only slightly less than that of the CC σ-bond, and this has been identified as one of the factors reponsible for the diverse and extensive chemistry of carbon.[4] The stabilizing features for the PS π-bond listed above represent a contribution toward general stable heteroatomic π-bonding, which is energetically competitive with the respective σ-bonding. Such a development has significant consequences in terms of the advancement of the chemistry of the non-metals as a whole. There is now potential for the synthesis of π-bonded systems containing many new combinations of the heavier non-metals.

Acknowledgment. We thank the Natural Sciences and Engineering Research Council of Canada (N.B. and T.S.C), the donors of the Petroleum Research Fund, administered by the American Chemical Society (N.B.), and Dalhousie University for financial support, Dr. D. L. Hooper and the Atlantic Regional Magnetic Resonance Center for obtaining the NMR spectra, and Patrick Cho for help in preparing (**1b**)$AlClBr_3$.

Supplementary Material Available: Tables SI-SVI, listing crystallographic data, anisotropic thermal parameters, bond lengths and angles, contact distances, torsion angles, and least-squares plane calculations for $C_6H_4PS_2^+$ $AlCl_4^-$ [(**1a**)$AlCl_4$] and $C_{13}H_{11}PS_2$ (**2c**), Table SIX, listing mass spectral and infrared data, and Figure S1, showing the contacts between anions and the cation (12 pages); Tables SVII and SVIII, listing observed and calculated structure factors (30 pages). Ordering information is given on any current masthead page.

Contribution from the Chemistry and Materials Science Divisions, Argonne National Laboratory, Argonne, Illinois 60439-4831, and Department of Chemistry, North Carolina State University, Raleigh, North Carolina 17695-8204

Synthesis of the New Organic Metal $(ET)_2C(CN)_3$ and Characterization of Its Metal-Insulator Phase Transition at ~180 K

Mark A. Beno,*[†] Hau H. Wang,[†] L. Soderholm,[†] K. Douglas Carlson,[†] L. N. Hall,[†] Luis Nuñez,[†] Helena Rummens,[†] Benjamin Anderson,[†] John A. Schlueter,[†] Jack M. Williams,[†] Myung-Hwan Whangbo,*[‡] and Michel Evain[‡]

Received March 17, 1988

A new conducting salt $(ET)_2C(CN)_3$, the first 2:1 salt of ET (i.e., bis(ethylenedithio)tetrathiafulvalene) with a planar-triangular anion, was synthesized, and its structure was determined by single-crystal X-ray diffraction. Crystal data for $(ET)_2C(CN)_3$ are as follows: monoclinic, $P2/a$, $Z = 2$; at 125 K/298 K, a = 14.684 (8)/14.979 (7) Å, b = 6.667 (3)/6.700 (2) Å, c = 16.400 (6)/16.395 (4) Å, β = 95.13 (3)/94.80 (3)°, and V_c = 1599 (1)/1639.7 (9) Å^3. The electrical conductivity of this salt as a function of temperature shows that it undergoes a metal-insulator phase transition at ~180 K. The magnetic susceptibility measured as a function of temperature and the tight-binding band electronic structure calculated for $(ET)_2C(CN)_3$ show that the phase transition at ~180 K is a Peierls type metal-insulator transition. The band electronic structure of $(ET)_2C(CN)_3$ predicts a doubling of the b axis as a consequence of the Peierls distortion, which has been confirmed by the use of X-ray photographs of $(ET)_2C(CN)_3$ taken as a function of temperature.

The donor molecule bis(ethylenedithio)tetrathiafulvalene (**1**). (BEDT-TTF or simply ET) is the source of numerous salts of type $(ET)_mX_n$ with mononegative ions X^-.[1] Of the several 2:1 salts

1

produced with linear anions, only the β-phase salts, β-$(ET)_2X$, with X^- = I_3^-, AuI_2^-, and IBr_2^- give rise to ambient-pressure superconductors (T_c = 1.4,[2] 5.0,[3] and 2.8 K[4] for X^- = I_3^-, AuI_2^-, and IBr_2^-, respectively). Recently, a 2:1 salt, $(ET)_2Cu(SCN)_2$, with a bent anion has been found to be an ambient-pressure superconductor, but with a much higher transition temperature (T_c = 10.4 K).[5] ET salts with planar-triangular anions are rare, the only examples being α, β, and γ phases with NO_3^-.[6] In the present study, we report the synthesis of $(ET)_2C(CN)_3$, the first 2:1 salt with a planar-triangular anion, and its crystal structure as determined by single-crystal X-ray diffraction. Electrical conductivity of $(ET)_2C(CN)_3$ measured as a function of temperature indicates that this salt undergoes a broad metal-insulator (MI) transition near 180 K. We have characterized this phase transition by measurements of the magnetic susceptibility and by

[†] Argonne National Laboratory.
[‡] North Carolina State University.

(1) Williams, J. M.; Wang, H. H.; Emge, T. J.; Geiser, U.; Beno, M. A.; Leung, P. C. W.; Carlson, K. D.; Thorn, R. J.; Schultz, A. J.; Whangbo, M.-H. *Prog. Inorg. Chem.* **1987**, *35*, 51.
(2) (a) Yagubskii, E. G.; Shchegolev, I. F.; Laukhin, V. N.; Kononovich, P. A.; Kartsovnik, M. V.; Zvarykina, A. V.; Buravov, L. I. *JETP Lett. (Engl. Transl.)* **1984**, *39*, 12. (b) Williams, J. M.; Emge, T. J.; Wang, H. H.; Beno, M. A.; Copps, P. T.; Hall, L. N.; Carlson, K. D.; Crabtree, G. W. *Inorg. Chem.* **1984**, *23*, 2558.
(3) Wang, H. H.; Beno, M. A.; Geiser, U.; Firestone, M. A.; Webb, K. S.; Nuñez, L.; Crabtree, G. W.; Carlson, K. D.; Williams, J. M.; Azevedo, L. J.; Kwak, J. F.; Schirber, J. E. *Inorg. Chem.* **1985**, *24*, 2465.
(4) Williams, J. M.; Wang, H. H.; Beno, M. A.; Emge, T. J.; Sowa, L. M.; Copps, P. T.; Behroozi, F.; Hall, L. N.; Carlson, K. D.; Crabtree, G. W.; *Inorg. Chem.* **1984**, *23*, 3839.
(5) (a) Urayama, H.; Yamochi, H.; Saito, G.; Nozawa, K.; Sugano, T.; Kinoshita, M.; Sato, S.; Oshima, K.; Kawamato, A.; Tanaka, J. *Chem. Lett.* **1988**, 55. (b) Urayama, H.; Yamochi, H.; Saito, G.; Sato, S.; Kawamoto, A.; Tanaka, A.; Mori, T.; Maruyama, Y.; Inokuchi, H. *Chem. Lett.* **1988**, 463. (c) Carlson, K. D.; Geiser, U.; Kini, A. M.; Wang, H. H.; Montgomery, L. K.; Kwok, W. K.; Beno, M. A.; Williams, J. M.; Cariss, C. S.; Crabtree, G. W.; Whangbo, M.-H.; Evain, M. *Inorg. Chem.* **1988**, *27*, 965.
(6) Weber, A.; Endres, H.; Keller, H. J.; Gogu, E.; Heinen, I.; Bender, K.; Schweitzer, D. *Z. Naturforsch* **1985**, *40B*, 1658.

0020-1669/89/1328-0150$01.50/0

Table I. Experimental Parameters for the X-ray Diffraction Study of $(ET)_2(C(CN)_3)$ at 125/298 K

space group $P2/a$ [No. 13]	Z = 2 formula units/unit cell
$(C_{10}H_8S_8)_2C(CN)_3$	λ = 0.71073 Å (Mo Kα radiation)
a = 14.684 (8)/14.979 (7) Å	M_r = 859.439
b = 6.667 (3)/6.700 (2) Å	ρ_c = 1.785 (1)/1.741 (1) g/cm^3
c = 16.400 (6)/16.395 (4) Å	μ_c = 10.66/10.40 cm^{-1}
β = 95.13 (3)/94.80 (3)°	T_{max} = 91.4/91.6%
V_{cell} = 1599 (1)/1639.7 (9) Å^3	T_{min} = 74.4/74.9%

	all data	data with $F_o^2 \geq 3\sigma(F_o^2)$
$R(F_o)^a$	0.053/0.051	0.047/0.045
$R_w(F_o)^b$	0.065/0.052	0.064/0.051

$^a R(F_o) = \sum||F_o| - |F_c||/\sum|F_o|$. $^b R_w(F_o) = [\sum w(|F_o| - |F_c|)^2/\sum wF_o^2]^{1/2}$.

calculations of the band electronic structure.

Synthesis

(PPN)C(CN)$_3$. Aqueous solutions of 4.24 g of (PPN)Cl (Alfa Products, 7.4 mmol) (PPN is the bis(triphenylphosphine)nitrogen(1+) ion) and 0.95 g of KC(CN)$_3$ (Alfa Products 7.4 mmol) were mixed at about 60 °C. The resulting white precipitate was dried in vacuum and recrystallized twice from CH_2Cl_2/diethyl ether to give 3.61 g of (PPN)C(CN)$_3$ (5.74 mmol, 78% yield). Anal. Calcd (found) for $C_{40}H_{30}N_4P_2$: C, 76.42 (76.01); H, 4.81 (4.75); N, 8.91 (9.47); P, 9.85 (10.28). Mp 168–169 °C.

(ET)$_2$C(CN)$_3$. A mixture of 9.8 mg of ET (Strem Chemicals, 1.7 mM) and 360 mg of (PPN)C(CN)$_3$ (38 mM) in THF were used for electrocrystallization. A current density of 1 μA/cm^2 was applied for 8 days to give 3.9 mg of black lustrous crystals of (ET)$_2$C(CN)$_3$ (36% yield) on the Pt anode. The room-temperature peak-to-peak ESR line width of these crystals is in the range 25–35 G. No other phases were detected on the basis of ESR line widths or X-ray diffraction measurements.

Crystal Structure

Crystals of $(ET)_2C(CN)_3$ were examined at 298 and 125 K on a Syntex $P2_1$ diffractometer equipped with a nitrogen cold-stream device. The unit cell parameters, as determined from setting angles of 25 reflections with $8° < 2\theta < 20°$ and verified by pseudorotation photographs, along with other crystallographic data are given in Table I. The reflection data were treated for Lorentz and polarization effects, and a Gaussian absorption correction[7] was applied. The crystal structure was solved with the program MULTAN 78[8] and refined by full-matrix least-squares methods to convergence (all shifts less than 0.1σ). Anisotropic thermal parameters were used for all non-hydrogen atoms. Hydrogen atoms were included at calculated positions (assuming ideal sp^3 geometry for the ethylene carbon atoms and a C–H distance of 1.0 Å), with U_{iso} = 0.04 and 0.06 Å^2 for the 125 and 298 K data, respectively. Atomic scattering factors with corrections for anomalous dispersion were obtained from the literature.[9] The atomic coordinates and equivalent isotropic thermal parameters are given in Table II, and the intramolecular distances and angles for the ET molecule and $C(CN)_3^-$ anion are listed in Table III. The atom numbering schemes for ET and the $C(CN)_3^-$ anions are shown in Figures 3 and 1, respectively.

The $C(CN)_3^-$ anion, shown in Figure 1, has the central carbon atom (C11) and one cyano group (C12–N12) located on a 2-fold axis. The intramolecular bond distances and angles as given in Table III are nearly identical with those observed in the NaC(CN)$_3$ salt.[10] No significant anion to donor interactions were observed.

Layers of ET molecules alternate with the $C(CN)_3^-$ anion layers along the c axis, as shown in Figure 2. The ET molecules are stacked in dimeric units along the crystallographic a axis with four ET molecules per repeat unit. The parallel ET molecules within the dimer units are separated by ~3.57 Å, and adjacent

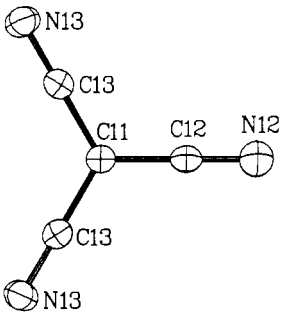

Figure 1. Atomic numbering scheme for the $C(CN)_3^-$ anion.

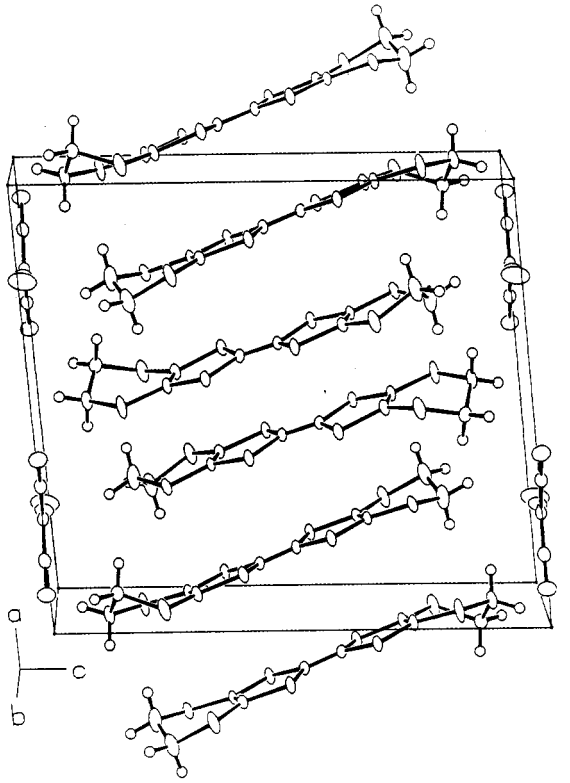

Figure 2. Unit cell diagram. The ET molecules in $(ET)_2C(CN)_3$ form a zigzag stack with no short intrastack S···S contacts (<3.6 Å, the van der Waals radii sum).

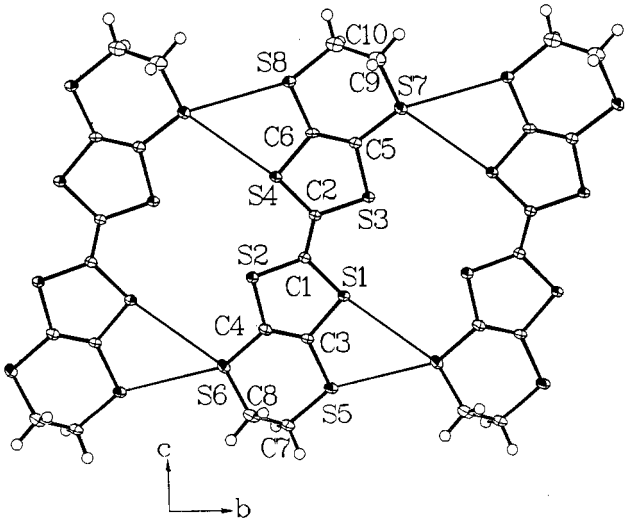

Figure 3. Short interstack S···S contacts linking the ET stacks to form a 2-dimensional sheet of ET molecules.

(7) Strouse, C. E. "UCLA Crystallographic Program Package", University of California, Los Angeles, 1978.
(8) Main, P.; Hall, S. E.; Lesinger, L.; Germain, G.; Declercq, J.-P.; Woolfson, M. M. "MULTAN78. A System of Computer Crystal Structures from X-Ray Diffraction Data", Universities of York, England, and Louvain, Belgium, 1978.
(9) *International Tables for X-Ray Crystallography*; Kynoch: Birmingham, England, 1978, Vol. IV.
(10) Andersen, P.; Klewe, B.; Thom, E. *Acta Chem. Scand.* **1967**, *21*, 1530.

Table II. Positional and Equivalent Isotropic Thermal Parameters[a] for $(ET)_2C(CN)_3$

atom	x	y	z	10^4U_{eq}, Å^2
		T = 125 K		
S1	0.55213 (4)	0.81397 (8)	0.35133 (3)	180 (1)
S2	0.58788 (4)	0.38806 (9)	0.38974 (3)	195 (1)
S3	0.63034 (4)	0.93412 (8)	0.53592 (3)	192 (1)
S4	0.65667 (4)	0.50572 (8)	0.57654 (3)	193 (1)
S5	0.48573 (6)	0.74843 (9)	0.17806 (4)	309 (2)
S6	0.52539 (6)	0.24353 (9)	0.22314 (4)	296 (2)
S7	0.69641 (5)	1.08624 (9)	0.69784 (4)	292 (2)
S8	0.72663 (4)	0.57545 (9)	0.75008 (3)	206 (2)
C1	0.58840 (15)	0.6349 (3)	0.42472 (12)	154 (5)
C2	0.61998 (15)	0.6853 (3)	0.50366 (12)	154 (5)
C3	0.5236 (2)	0.6408 (3)	0.27255 (12)	180 (6)
C4	0.5392 (2)	0.4446 (4)	0.29114 (13)	196 (6)
C5	0.6740 (2)	0.8760 (3)	0.63618 (13)	167 (5)
C6	0.68557 (15)	0.6786 (3)	0.65547 (12)	155 (5)
C7	0.4841 (2)	0.5395 (4)	0.10692 (14)	245 (6)
C8	0.5508 (2)	0.3715 (4)	0.1298 (2)	243 (6)
C9	0.7591 (2)	0.9787 (5)	0.7867 (2)	382 (9)
C10	0.7222 (3)	0.7879 (5)	0.8173 (2)	415 (10)
C11	0.7500 (0)	0.0875 (5)	1.0000 (0)	201 (8)
C12	0.7500 (0)	0.2985 (6)	1.0000 (0)	296 (11)
N12	0.7500 (0)	0.4722 (7)	1.0000 (0)	546 (16)
C13	0.6665 (2)	−0.0190 (4)	0.99646 (14)	225 (6)
N13	0.5987 (2)	−0.1094 (4)	0.9943 (2)	331 (7)
		T = 298 K		
S1	0.54927 (5)	0.80955 (10)	0.35192 (4)	412 (2)
S2	0.58764 (5)	0.38865 (10)	0.38902 (4)	427 (2)
S3	0.62948 (5)	0.93077 (10)	0.53437 (4)	441 (2)
S4	0.65560 (5)	0.50663 (10)	0.57485 (4)	410 (2)
S5	0.48508 (7)	0.74462 (11)	0.17961 (4)	590 (3)
S6	0.52951 (6)	0.24478 (11)	0.22277 (4)	558 (3)
S7	0.70207 (8)	1.08214 (11)	0.69286 (5)	703 (3)
S8	0.72884 (5)	0.57785 (10)	0.74580 (4)	458 (2)
C1	0.5888 (2)	0.6334 (4)	0.42397 (14)	331 (7)
C2	0.6204 (2)	0.6838 (4)	0.50189 (14)	337 (7)
C3	0.5239 (2)	0.6383 (4)	0.27303 (14)	358 (8)
C4	0.5412 (2)	0.4446 (4)	0.29059 (14)	365 (8)
C5	0.6764 (2)	0.8735 (4)	0.63289 (14)	376 (8)
C6	0.6875 (2)	0.6782 (4)	0.65213 (14)	340 (7)
C7	0.4825 (3)	0.5403 (5)	0.1093 (2)	620 (12)
C8	0.5471 (2)	0.3722 (5)	0.1288 (2)	591 (11)
C9	0.7458 (4)	0.9791 (6)	0.7859 (2)	974 (19)
C10	0.7311 (4)	0.7899 (6)	0.8097 (2)	1059 (22)
C11	0.7500 (0)	0.0876 (7)	1.0000 (0)	483 (14)
C12	0.7500 (0)	0.2948 (9)	1.0000 (0)	793 (22)
N12	0.7500 (0)	0.4640 (9)	1.0000 (0)	1575 (40)
C13	0.6682 (2)	−0.0160 (5)	0.9972 (2)	559 (11)
N13	0.6021 (2)	−0.1037 (5)	0.9952 (2)	873 (14)

[a] The complete temperature factor is $\exp[-U_{eq}(8\pi^2(\sin^2\theta)/\lambda^2)]$ where $U_{eq} = {}^1/_3\sum_i\sum_j U_{ij}a^*_i a^*_j \mathbf{a}_i\cdot\mathbf{a}_j$.

dimer units are rotated by approximately 30° with respect to the long axis of the ET molecule. No intrastack S···S intermolecular contact distances are less than the van der Waals radii sum of 3.6 Å; however, as shown in Figure 3, short interstack intermolecular S···S contacts are observed.

The ethylene groups of the ET molecule are not contained in the molecular π-framework, and thus their arrangement can be either eclipsed or staggered when viewed along the long molecular axis.[11] For an isolated ET molecule the two arrangements of the ethylene groups would be similar in energy, but this is not the case for ET salts due to donor–anion interactions resulting from the hydrogen anion contacts.[11] In $(ET)_2C(CN)_3$ the ET molecules have a staggered arrangement of ethylene groups, as shown in Figure 2.

Metal–Insulator Phase Transition

The ESR peak-to-peak line width and spin susceptibility of a single crystal of $(ET)_2C(CN)_3$ measured as a function of temperature[12] from 300 to 100 K are shown in Figure 4. In the temperature region 300–200 K, the line width decreased very slightly with decreasing temperature and the spin susceptibility is constant down to 220 K. This behavior is consistent with Pauli paramagnetism for a metallic conductor. Below 200 K, both the line width and the spin susceptibility drop significantly, indicating typical behavior for a metal–insulator (MI) transition. Similar changes in the ESR line width and spin susceptibility have been

Table III. Distances (Å) and Angles (deg) for $(ET)_2C(CN)_3$ at 125 K

A. The ET Molecule

Distances

S1–C1	1.745 (2)	S1–C3	1.755 (2)	S2–C1	1.742 (2)
S2–C4	1.750 (2)	S3–C2	1.744 (2)	S3–C5	1.754 (2)
S4–C2	1.743 (2)	S4–C6	1.756 (2)	S5–C3	1.752 (2)
S5–C7	1.816 (2)	S6–C4	1.744 (2)	S6–C8	1.820 (3)
S7–C5	1.742 (2)	S7–C9	1.801 (3)	S8–C6	1.754 (2)
S8–C10	1.799 (3)	C1–C2	1.377 (3)	C3–C4	1.358 (3)
C5–C6	1.361 (3)	C7–C8	1.513 (4)	C9–C10	1.487 (4)

Angles

C1–S1–C3	95.49 (11)	C1–S2–C4	95.17 (11)
C2–S3–C5	95.10 (10)	C2–S4–C6	95.40 (10)
C3–S5–C7	103.83 (11)	C4–S6–C8	99.00 (12)
C5–S7–C9	101.87 (13)	C6–S8–C10	101.83 (13)
C2–C1–S2	122.10 (17)	C2–C1–S1	122.53 (17)
S2–C1–S1	115.29 (12)	C1–C2–S4	122.30 (17)
C1–C2–S3	122.04 (17)	S4–C2–S3	115.61 (12)
C4–C3–S5	128.80 (17)	C4–C3–S1	116.36 (16)
S5–C3–S1	114.68 (13)	C3–C4–S6	126.11 (17)
C3–C4–S2	117.51 (16)	S6–C4–S2	116.09 (14)
C6–C5–S7	129.05 (17)	C6–C5–S3	117.33 (16)
S7–C5–S3	113.62 (13)	C5–C6–S8	127.64 (16)
C5–C6–S4	116.51 (15)	S8–C6–S4	115.85 (12)
C8–C7–S5	115.92 (17)	C7–C8–S6	112.23 (18)
C10–C9–S7	116.00 (23)	C9–C10–S8	115.63 (22)

B. The $C(CN)_3^-$ Anion

Distances

C11–C12	1.407 (5)	C11–C13	1.413 (3)	C12–N12	1.158 (6)
C13–N13	1.161 (3)				

Angles

C12–C11–C13	120.15 (16)	C13–C11–C13	119.70 (32)
N12–C12–C11	180.00 (0)	N13–C13–C11	178.75 (28)

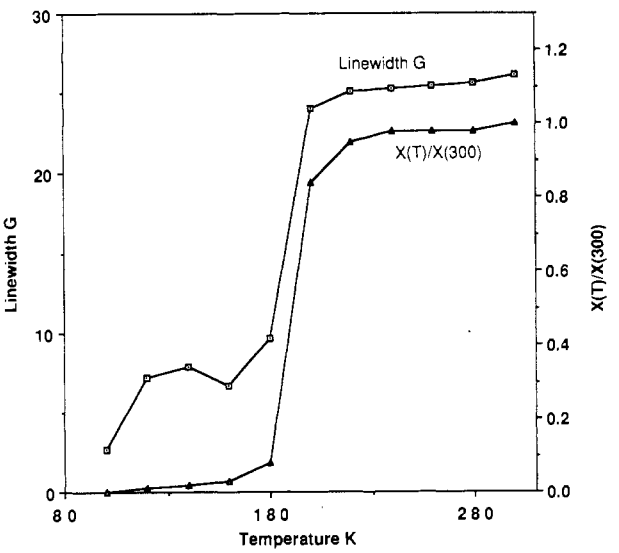

Figure 4. Variation in ESR line width and spin susceptibility with temperature for $(ET)_2C(CN)_3$.

(11) Whangbo, M.-H.; Williams, J. M.; Schultz, A. J.; Emge, T. J.; Beno, M. A. *J. Am. Chem. Soc.* **1987**, *109*, 90.

(12) The ESR spectra were recorded by employing an IBM ER 200D-SRC X-band spectrometer (9.5 GHz), equipped with a rectangular cavity operating in the TE_{102} mode. The temperature was controlled from 30 to 297 K with an Oxford Instrument EPR-900 flow cryostat with an ITC4 temperature controller.

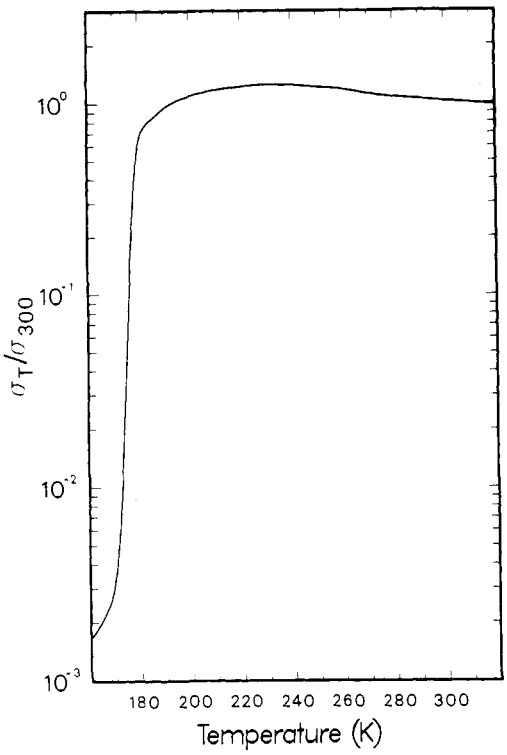

Figure 5. Relative conductivity of $(ET)_2C(CN)_3$ as a function of temperature. This figure shows a metal–insulator transition near 230 K.

observed previously at the MI transition in α-$(ET)_2I_3$.[13]

The electrical conductivity of $(ET)_2C(CN)_3$ was measured as a function of temperature by use of the four-probe technique with low-frequency ac current and phase-sensitive detection. The probes consisted of gold wires, attached with gold conducting paste, aligned along the *a* axis, which is the stacking axis of the ET molecules and also the axis of highest electrical conductivity. The measurements carried out on several different crystal specimens yielded similar results. The temperature dependence of the conductivity is shown in Figure 5. A metallic behavior is observed from room temperature to ~230 K. Within this range, the conductivity slightly increases with decreasing temperature, to a value at 230 K that is 1.14 times larger than that of the room-temperature value. From the crystal dimensions and voltage probe distances we estimate that $\sigma \simeq 1\ (\Omega\ cm)^{-1}$ at 300 K. Thus, the metallic nature of this salt is not very pronounced from the standpoint of both its conductivity and temperature dependence. Near 230 K, the salt undergoes a metal–insulator transition: the conductivity decreases initially very slowly below 230 K but drops rapidly at ~180 K.

The magnetic susceptibility of $(ET)_2C(CN)_3$ as a function of temperature[14] is shown in Figure 6. A diamagnetic correction of $\sim 426 \times 10^{-6}$ emu/mol was calculated by using Pascal's constants[15] and has been applied to the data. The rapid increase in the susceptibility at 175 (2) K corresponds to the onset of the rapid rise in the conductivity observed upon increasing temperature; see Figure 4. This magnetic behavior, as well as conductivity, ESR, and structural measurements are consistent with a Peierls metal–insulator transition[16] at about 175 K. Below the phase-transition temperature, the susceptibility falls to zero, and the material is diamagnetic, unlike the Bechgaard salts, which have a transition

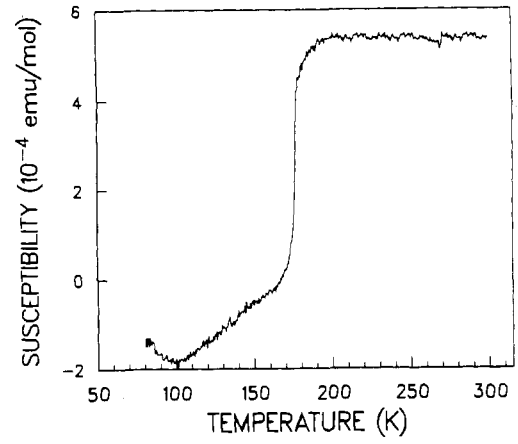

Figure 6. Magnetic susceptibility measurements of $(ET)_2C(CN)_3$ showing normal Pauli paramagnetism above 175 (2) K and the occurrence of diamagnetic behavior at lower temperatures.

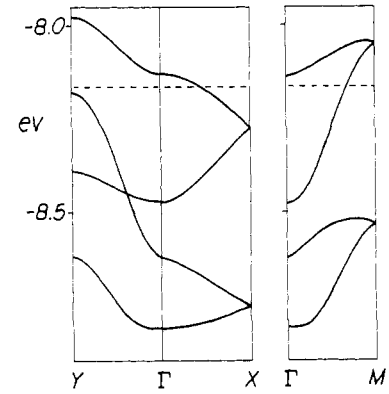

Figure 7. Dispersion relations of the top two occupied bands of $(ET)_2C(CN)_3$ where the dashed line is the Fermi level. $\Gamma = (0, 0, 0)$, $X = (a^*/2, 0, 0)$, $Y = (0, b^*/2, 0)$, $M = (a^*/2, b^*/2, 0)$.

to a magnetically ordered (SDW) ground state at low temperatures.[17,18]

Above 175 K, $\chi_{exptl} = 5.4 \times 10^{-4}$ emu/mol and is temperature-independent; this is very unusual for organic conductors, which normally show a marked temperature dependence for their susceptibility well above a phase transition. The temperature-independent behavior is attributable to metallic, Pauli paramagnetism. Assuming a tight-binding model, the susceptibility of noninteracting spins may be calculated from[19,20]

$$\chi_p = \frac{N_c \mu_B^2}{\pi |t| \sin(\pi\rho/2)}$$

where μ_B is the Bohr magneton, $|t|$ is the transfer or resonance integral, and ρ is the number of electrons transferred per ET molecule. Since the cation/anion ratio is 2:1, and full charge transfer is expected, a value of $\rho = 0.5$ is assumed. If a value of the transfer integral, $|t| = 0.16$, as determined by analysis of the near-infrared data[21] for β-$(ET)_2IBr_2$ and β-$(ET)_2I_3$, is assumed, then $\chi_p = 1.7 \times 10^{-4}$. This calculated susceptibility is a factor of 3.2 smaller than the measured value of 5.4 emu/mol. A similar enhancement of the experimental susceptibility over the tight-binding model calculated paramagnetism has also been reported for TCNQ salts,[20] $(ET)_3(ClO_4)_2$,[22] and α-$(ET)_2I_3$.[23] This en-

(13) Venturini, E. L.; Azevedo, L. J.; Schirber, J. E.; Williams, J. M.; Wang, H. H. *Phys. Rev. B: Condens. Matter* **1985**, *32*, 2819.
(14) Magnetic susceptibility data were obtained with a George Associates Lewis Coil force magnetometer. Fields were varied to 6000 Oe, measured with a precalibrated Hall probe. Temperatures over the range $4 < T < 300$ K were monitored by a Ni–Cr vs Cu–Ni (chromel–constantan) thermocouple.
(15) Selwood, P. W. *Magnetochemistry*; Interscience: London, 1979; p 435.
(16) (a) Peierls, R. E. *Quantum Theory of Solids*; Oxford University Press: London, 1955; p 108. (b) Berlinsky, A. *Contemp. Phys.* **1976**, *17*, 331. (c) Whangbo, M.-H. *Acc. Chem. Res.* **1983**, *16*, 95.
(17) Scott, J. C.; Pedersen, H. J.; Bechgaard, K. *Phys. Rev. Lett.* **1980**, *45*, 2125.
(18) Mortensen, K.; Tomkiewicz, Y.; Schultz, T. D.; Engler, E. M. *Phys. Rev. Lett.* **1981**, *46*, 1234.
(19) Torrance, J. B.; Tomkiewicz, Y.; Silverman, B. D. *Phys. Rev. B: Condens. Matter* **1977**, *15*, 4738.
(20) Jerome, D.; Schultz, H. J. *Adv. Phys.* **1982**, *31*, 299.
(21) Sugano, T.; Saito, G. *J. Phys. C:* **1986**, *B34*, 1485.
(22) Parkin, S. S. P.; Miljak, M.; Cooper, J. S. *Phys. Rev. B: Condens. Matter* **1986**, *34*, 1485.

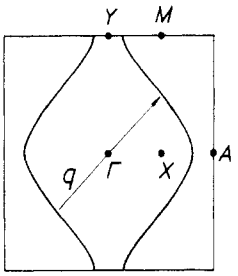

Figure 8. Fermi surface associated with the half-filled band of Figure 7. The wave vectors of the region including Γ surrounded by the two curves lead to filled band levels, while those of the other region lead to empty band levels. Here $A = (a^*, 0, 0)$.

hancement has been attributed to strong electron–electron interaction and treated by using a modified Hubbard model,[19] which corrects for the on-site repulsion of two electrons. However, recent work suggests that the enhancement of χ_ρ is most strongly dependent on the degree of charge transfer, ρ.[24] The enhancement observed for $(ET)_2C(CN)_3$, $\chi_\rho/\chi_{exptl} = 3.2$ for $\rho = 0.5$, agrees well with the latter explanation.

Band Electronic Structure

To understand the origin of the metal–insulator transition of $(ET)_2C(CN)_3$ at ~175 K, we performed tight-binding band calculations[1,25] based upon the extended Hückel method.[26] Figure 7 shows the dispersion relations of the top two occupied bands of $(ET)_2C(CN)_3$, where the dashed line indicates the Fermi level. These bands are mainly derived from the HOMO's of four ET molecules in every unit cell. With the formal oxidation of two $(ET)_2^+$ per unit cell, the upper band is half-filled. The Fermi surface associated with this band is shown in Figure 8, where an extended Brillouin zone scheme is used due to the folded nature of each band in Figure 7. The Fermi surface of Figure 8 shows a good nesting with the vector $\mathbf{q} \simeq a^* + b^*/2$. The presence of the $b^*/2$ component in the nesting vector suggests that $(ET)_2C(CN)_3$ would undergo a Peierls distortion that doubles the b axis, which would be the origin of the metal–insulator phase transition at ~175 K. These predictions were verified by very long X-ray axial photographs of $(ET)_2C(CN)_3$ at 125 K, which revealed the presence of a b-axis doubling as anticipated.

Concluding Remarks

$(ET)_2C(CN)_3$, synthesized and characterized in the present work, is the first 2:1 salt of ET with a planar-triangular anion. The electrical properties of this salt measured as a function of temperature show that it undergoes a metal-insulator phase transition at ~180 K. The magnetic susceptibility measured as a function of temperature and the tight-binding band electronic structure calculated for $(ET)_2C(CN)_3$ lead to the conclusion, as confirmed by X-ray diffraction observations, that the metal–insulator phase transition is caused by a Peierls transition which results from the doubling of the b axis.

Acknowledgment. Work at North Carolina State University and Argonne National Laboratory was supported by the U.S. Department of Energy, Office of Basic Energy Sciences, Divisions of Materials Sciences and Chemical Sciences, under Grant DE-FG-05-86-ER45259 and under Contract W31-109-ENG-38, respectively. We express our appreciation for computing time made available by DOE on the ER-Cray X-MP computer. B.A. and J.A.S. are student research participants sponsored by the Argonne Division of Educational Programs from Wittenberg University, Springfield, OH, and Valparaiso University, Valparaiso, IN, respectively.

Supplementary Material Available: Tables of complete crystallographic data and anisotropic thermal parameters at 125 and 298 K (3 pages); tables of observed and calculated structure factors at 125 and 298 K (24 pages). Ordering information is given on any current masthead page.

(23) Rothaemel, B.; Forro, L.; Cooper, J. R.; Schilling, J. S.; Weger, M.; Bele, P.; Brunner, H.; Schweitzer, D.; Keller, H. J. *Phys. Rev. B: Condens. Matter* **1986**, *34*, 704.
(24) Mazumdar, S.; Dixit, S. N. *Phys. Rev. B: Condens. Matter* **1986**, *34*, 3683.
(25) Whangbo, M.-H.; Williams, J. M.; Leung, P. C. W.; Beno, M. A.; Emge, T. J.; Wang, H. H.; Carlson, K. D.; Crabtree, G. W. *J. Am. Chem. Soc.* **1985**, *107*, 5815.
(26) Hoffmann, R. *J. Chem. Phys.* **1983**, *39*, 1397.

Contribution from the Department of Chemistry, National Tsing Hua University, Hsinchu, ROC, and Institute of Atomic and Molecular Sciences, Academia Sinica, Taipei, P.O. Box 23-166, Taiwan, ROC

Homogeneous Coprecipitation as a Means toward High-T_c and Sharp-Transition $YBa_2Cu_3O_{7-x}$ Superconducting Oxides[1]

R. S. Liu,[2] C. T. Chang,* and P. T. Wu†

Received May 12, 1988

$YBa_2Cu_3O_{7-x}$ superconducting powders have been prepared from an aqueous solution that contains Y, Ba, and Cu salts and oxalic acid via homogeneous coprecipitation using urea. The dried precipitate was found to have a stoichiometry as desired and a particle size of 0.3 ± 0.08 μm that has a specific surface area of 5.3 m^2/g. Subsequent calcination at 900 °C for 16 h and sintering at 950 °C for 16 h yielded a good superconductor with high reproducibility. The resulting powder has a T_c at 93 K with a sharp-transition width of $\Delta T = 1$ K. This process can be employed in a large-scale preparation of the $YBa_2Cu_3O_{7-x}$ powder.

Introduction

Solid-state reactions are the most commonly adopted processes for the preparation of high-T_c superconducting ceramics such as $YBa_2Cu_3O_{7-x}$.[3] These methods, usually, involve a series of laborious cycles of heating and grinding with an unavoidable compositional inhomogeneity. In order to attain higher homogeneity and also better control of stoichiometry, coprecipitation has been employed by various workers.[4-7] Kini et al.[5] used K_2CO_3 as the

* To whom correspondence should be addressed at Academia Sinica.
† Present address: Materials Research Laboratories, Industrial Technology Research Institute, Chutung, Hsinchu, Taiwan, ROC.

(1) Partially presented at the Materials Research Society spring meeting, Reno, NV, April 5-8, 1988.
(2) Also affiliated with Materials Research Laboratories, ITRI.
(3) Cava, R. J.; Batlogg, B.; van Dover, R. B.; Murphy, D. W.; Sunshine, S.; Siegrist, T.; Remeika, J. P.; Rietman, E. A.; Zahurak, S.; Espinosa, G. P. *Phys. Rev. Lett.* **1987**, *58*, 1676-1679.

0020-1669/89/1328-0154$01.50/0